

# Mapping the Properties of Low-Frequency Microseisms for Seismic Hazard Assessment

A. A. Lyubushin

*Schmidt Institute of Physics of the Earth, Russian Academy of Sciences, ul. B. Gruzinskaya 10, Moscow, 123995 Russia*

Received May 26, 2012

**Abstract**—The structure of low-frequency seismic noise in the range of periods from 2 min to 500 min is studied from the data of continuous seismic monitoring at 77 seismic stations of the F-net broadband network in Japan from the beginning of 1997 to May 15, 2012. A new statistical characteristic of seismic noise is suggested, namely, the minimal normalized entropy  $En$  of the distribution of squared orthogonal wavelet coefficients. This parameter of seismic noise is analyzed in conjunction with the multifractal statistics—the support width of the singularity spectrum,  $\Delta\alpha$ , and the generalized Hurst exponent,  $\alpha^*$ , which were extensively used by the author in the previous works for analyzing the low-frequency seismic noise. The method for constructing the maps of spatial distribution of  $\Delta\alpha$ ,  $\alpha^*$ ,  $En$ , and their aggregated normalized value over the time windows with a given length is proposed. The maps are constructed by averaging the succession of the elementary charts, each of which corresponds to a day of observations. It is shown that, for the islands of Japan, the reduction in  $\Delta\alpha$  and  $\alpha^*$  and the increase in  $En$  outline the area of the forthcoming mega earthquake of March 11, 2011, with  $M = 9$  (Tohoku earthquake). According to the analysis of about a year's worth of data after this event, the region south of Tokyo (Nankai trough) is still dominated by decreased  $\Delta\alpha$  and  $\alpha^*$  and increased  $En$ . This gives grounds to hypothesize that this region remains at a high level of seismic threat since the accumulated stresses were incompletely released by the Tohoku earthquake. Drawing an analogy to the behavior of the coefficient of correlation between  $\Delta\alpha$  and  $\alpha^*$ , we may suppose that there is an increased probability of a strong earthquake occurring in the second half of 2013 or the first half of 2014. Constructing the averaged maps of the distributions of seismic noise parameters and their aggregated value in a moving time window is suggested as a new method for dynamical assessment of seismic hazards.

DOI: 10.1134/S1069351313010084

## INTRODUCTION

Low-frequency seismic noise is an important source of information about the processes occurring in the Earth's crust despite the fact that most of the energy of these vibrations is provided by the processes in the atmosphere and ocean such as variations in air pressure and the sea wave impacts on the shore and the shelf. The relationship between the low-frequency microseisms ranging in period from 5 to 500 s and the intensity of oceanic waves is thoroughly investigated in (Berger, Davis, and Ekstrom, 2004; Kobayashi and Nishida, 1998; Rhie and Romanowicz, 2004; Tanimoto et al., 1998; Tanimoto and Um, 1999; Ekstrom, 2001; Tanimoto, 2001; 2005). The Earth's crust serves as the propagation medium for the energy of the atmospheric and oceanic processes, and since the transfer properties of the crust depend on its state, the statistical properties of the microseisms reflect the variations in the properties of the lithosphere, including the changes preceding strong earthquakes.

The features of the periodic structure of the point process formed by the sharp spikes and asymmetric low-frequency pulses of microseismic noise before strong earthquakes were analyzed in (Sobolev, 2004; 2008; 2011; Sobolev, Lyubushin, and Zakrzhevskaya,

2005; 2008; Sobolev and Lyubushin, 2006). The effects of linear coherence in the variations of multifractal singularity spectra calculated from the waveforms of seismic noise at various stations were analyzed using the canonical correlations and coherence parameters in the moving time windows in (Lyubushin and Sobolev, 2006; Sobolev and Lyubushin, 2007a; 2007b; Lyubushin, 2007; 2008a).

The present work continues the series of previous publications (Lyubushin, 2009; 2010a; 2010b; 2011a; 2011b; 2011c) in which the prognostic properties of a variety of parameters of low-frequency seismic noise were analyzed from the records at the F-net broadband seismic network in Japan. The very first finding of these works was the detection of a statistically significant reduction in the average value (both over the entire set of the stations and over various groups of stations) of the support width of singularity spectrum  $\Delta\alpha$  after the earthquake of September 25, 2003 ( $M = 8.3$ ) off the shore of Hokkaido (Lyubushin, 2008b; 2009; 2010c). It was found that this phenomenon of a loss of multifractality could be interpreted as a manifestation of a general effect of nonlinear coherence in the temporal variations of the parameters of various systems as they approach the catastrophe (Pavlov and Anischenko, 2007). On this basis, it was hypothesized that the reduc-

tion in the average value of  $\Delta\alpha$  was a precursor to a strong earthquake with the magnitude  $M > 8.3$  in Japan, for which the earthquake of September 25, 2003, was sort of a foreshock. This finding was reported at the 7th General Assembly of the Asian Seismological Commission in Tsukuba, Japan, at the end of November 2008 (Lyubushin, 2008c).

Further, as new data became available and other statistics of the microseismic background were introduced in the joint analysis (Lyubushin, 2010a; 2010b), new results pointing to the synchronization of the parameters of microseismic noise (the onset of the synchronization was dated to the middle 2002) and, thus, to the increased seismic threat were obtained. The analysis of the pattern of correlation between the multifractal parameters  $\Delta\alpha$  and the generalized Hurst exponent  $\alpha^*$  (Lyubushin, 2011a, submitted April 2010) suggested that, starting from 2010, the islands of Japan entered the crucially hazardous stage of the seismic process. Thus, the prediction of the catastrophe, initially with the estimate for the magnitude only (issued in the middle of 2008) and then with the estimate for the expected time of the earthquake (presented in the middle of 2010), was published well ahead of the target event in a series of the mentioned papers and presentations at international conferences (Lyubushin, 2008c; 2010c; 2010e). This prediction was also documented in the proposal submitted on April 26, 2010, to the Russian Expert Council on Earthquake Prediction and Seismic Hazard Assessment.

After the earthquake of March 11, 2011, in Japan, the experience in its prediction was post factum described in detail in (Lyubushin, 2011b; 2011c). In (Lyubushin, 2011c), it was retrospectively shown that the approach applied indeed outlined the region of the forthcoming earthquake as a region marked with reduced values of  $\Delta\alpha$  on the map reflecting the spatial distribution of this parameter. It was found that the initial area with the low values  $\Delta\alpha$  split into southern and northern segments after the event of September 25, 2003. The northern segment, which includes central Japan on Honshu Island and the adjacent water area of the Pacific, became an epicentral zone and the area of aftershocks of the mega earthquake of March 11, 2011 (the Tohoku event).

After the Tohoku earthquake, the average level of  $\Delta\alpha$  on the islands of Japan increased sharply. As the F-net resumed its operations shortly after the event on March 14, 2011, the possibility appeared of monitoring the evolution of the properties of seismic noise after the mega earthquake by downloading and processing new data every two weeks. Even the first few months of measurements revealed the fact that the values of  $\Delta\alpha$  became maximal just in the zone of the epicenter and aftershocks of the earthquake of March 11, 2011, whereas the southern segment of the territory adjacent to Tokyo in the south within the Nankai trough remained dominated by relatively low  $\Delta\alpha$ . This was interpreted as a continuing seismic hazard in the south-

ern part of the region; moreover, the size of the zone dominated by the decreased  $\Delta\alpha$  suggests that this area could be hit by a new mega earthquake that is commensurate in energy with the Tohoku event of March 11, 2011 (Lyubushin, 2011d; Lyubushin, Rodkin, and Tikhonov, 2011).

The experiences in constructing the spatial distribution maps of different statistical characteristics of seismic noise indicate that, besides the mentioned statistical parameters, potentially seismically hazardous areas can also be revealed in the distributions of the other statistical characteristics of microseismic noise as anomalous areas with decreased or increased values of these parameters. Below, it is suggested, besides analyzing the support width of the singularity spectrum  $\Delta\alpha$ , to use also the other parameters of the seismic noise, including the generalized Hurst exponent  $\alpha^*$ . It was unexpectedly found that the normalized entropy of the distribution of squared wavelet coefficients  $En$ , which is a by-product in the procedure of selecting the best basis with a compact support, is also suitable for identifying the hazardous zones. Therefore, the comparison and combined use of these characteristics of seismic noise is of significant value for the research on seismic hazard assessment from the data of geophysical monitoring.

## THE DATA

The data recorded by the F-net broadband seismic network in Japan provided the input to this study. The network consisting of 83 stations has been continuously operating since 1997. The data from this network are freely accessible at <http://www.fnet.bosai.go.jp/top.php?LANG=en>. Figure 1 illustrates the layout of 77 F-net stations used in the present analysis. Six stations located on small remote islands south of 30° N were excluded from consideration. For this analysis, we downloaded the initial records of vertical components sampled at 1 Hz (LHZ records), which were then decimated to a sampling interval of 1 min by calculating the averages within successive time windows 60 points in length.

## THE STATISTICS USED

### The Minimal Normalized Entropy of the Wavelet Coefficient of Seismic Noise $En$

Below, we introduce the normalized entropy of the distribution of squared coefficients for the “best” orthogonal wavelet. In contrast to classical Fourier analysis, the wavelet processing of the signals raises the problem of selecting the basis. Most frequently, this basis is selected by the criterion of minimal entropy of the wavelet coefficient distribution (Mallat, 1998). Let  $X(t)$  be a finite sample of a random signal and  $t = 1, \dots, N$  be the index numerating the successive counts (the discrete time). The normalized entropy of the finite sample is defined by the following formula:

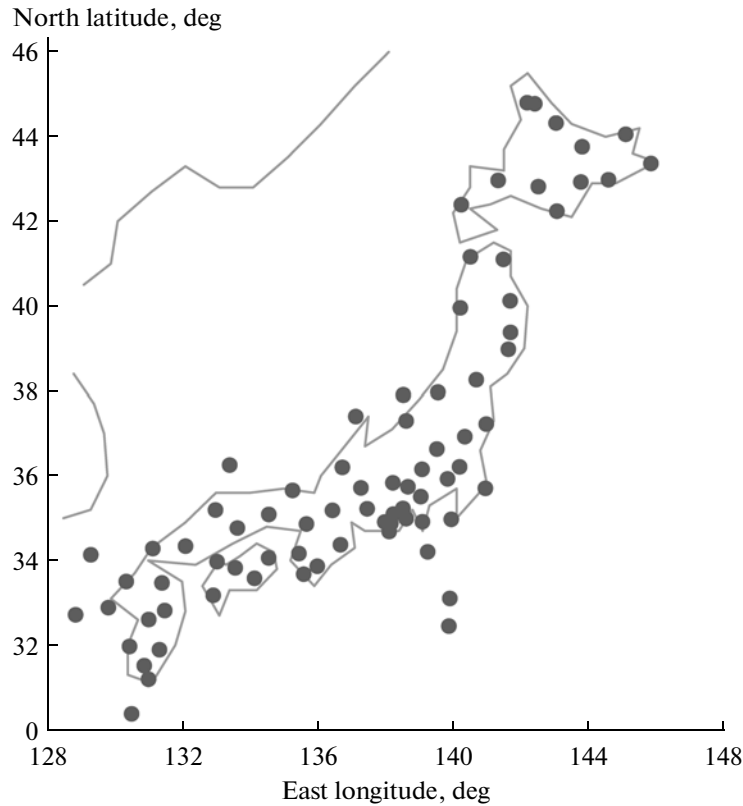


Fig. 1. Geometry of the broadband F-net seismic network in Japan.

$$En = -\sum_{k=1}^N p_k \log(p_k) / \log(N), \quad p_k = c_k^2 / \sum_{j=1}^N c_j^2, \quad (1)$$

$$0 \leq En \leq 1.$$

Here,  $c_k, k = 1, N$ , are the coefficients of the orthogonal wavelet representation with a certain basis. In the analysis described below, we used 17 Daubechies orthogonal wavelets: ten ordinary bases with the minimal support with one to ten vanishing moments and seven so-called Daubechies symlets (Mallat, 1998) with four to ten vanishing moments. For each basis, the normalized entropy of the distribution of squared coefficients was calculated by formula (1), and the basis rendering the minimum of (1) was determined. We note that, as the wavelets are the orthogonal transform, the sum of their squared coefficients is equal to the variance (energy) of the signal  $X(t)$ . Therefore, quantity (1) describes the entropy of the oscillation energy distribution on various spatial and temporal scales.

Selecting the basis by the criterion of minimal entropy relies on the idea that, in the case of minimal entropy, the maximum information about the signal is contained in the minimum number of wavelet coefficients that have quite large magnitudes. The minimum value of normalized entropy  $En$  emerges as a by-product of the solution to the problem of selecting the basis.

It turned out that this value has a series of properties that are of interest for geophysical interpretation.

Below, the value  $En$  was estimated in a moving time window that had a fixed length (1440 neighboring points of minute counts, which totals one day). Here, before calculating the normalized entropy (1), we detrended the data by an eighth-order polynomial fitting in order to eliminate the trends caused by tidal and thermal deformations of the Earth's crust and to pass to analyzing the characteristics of the noise. Thus, for each station, we formed a time series of minimal normalized entropy  $En, 0 \leq En \leq 1$  with a time step of one day.

### The Multifractal Parameters $\Delta\alpha$ and $\alpha^*$

We consider a certain random oscillation  $X(t)$  over the time interval  $[t - \delta/2, t + \delta/2]$ , which has the length  $\delta$  and is centered at the time point  $t$ . We examine the peak-to-peak amplitude  $\mu(t, \delta)$  of a random oscillation on this interval, i.e., the difference between the maximum and minimum  $X$ :

$$\mu(t, \delta) = \max_{t-\delta/2 \leq s \leq t+\delta/2} X(s) - \min_{t-\delta/2 \leq s \leq t+\delta/2} X(s). \quad (2)$$

If  $\delta \rightarrow 0$ , then  $\mu(t, \delta)$  will also tend to zero; however, it is the rate of this decay that is of importance for our analysis. If the decay rate follows the law  $\delta^{h(t)}$ :

$\mu(t, \delta) \sim \delta^{h(t)}$  or if there exists the limit  $h(t) = \lim_{\delta \rightarrow 0} \frac{\log(\mu(t, \delta))}{\log(\delta)}$ , then the value  $h(t)$  is referred to as the Helder–Lipschitz exponent. If  $h(t)$  does not depend on the time instant  $t$ ,  $h(t) = \text{const} = H$ , then the random oscillation  $X(t)$  is referred to as a monofractal oscillation and  $H$  is the Hurst exponent. If, finally, the Helder–Lipschitz exponents  $h(t)$  differ significantly for different instants of time  $t$ , the random oscillation is referred to as a multifractal, and for this oscillation, the notion of a singularity spectrum  $F(\alpha)$  can be defined (Feder, 1988). To do this, we mentally select a set  $C(\alpha)$  of such time instants  $t$  that have the same value of the Helder–Lipschitz exponent  $\alpha$ :  $h(t) = \alpha$ . The sets  $C(\alpha)$  exist (i.e., they contain certain elements and are not empty) for not all values of  $\alpha$ ; i.e., there exist some minimal  $\alpha_{\min}$  and maximal  $\alpha_{\max}$  such that the sets  $C(\alpha)$  are not empty only for  $\alpha_{\min} < \alpha < \alpha_{\max}$ . The multifractal singularity spectrum  $F(\alpha)$  is the fractal dimension of the set of the points  $C(\alpha)$ . The parameter  $\Delta\alpha = \alpha_{\max} - \alpha_{\min}$ , which is referred to as the singularity spectrum support width, is the most important multifractal characteristic. In addition, the argument  $\alpha^*$ , which renders the maximum of the singularity spectrum  $F(\alpha^*) = \max_{\alpha_{\min} \leq \alpha \leq \alpha_{\max}} F(\alpha)$ , is also of considerable interest. This parameter is the generalized Hurst exponent. The maximum of the singularity spectrum cannot exceed the dimension of the embedding set or the time axis,  $1, 0 < F(\alpha^*) \leq 1$ . Typically,  $F(\alpha^*) = 1$ . We note that, in the case of a monofractal signal,  $\Delta\alpha = 0, \alpha^* = H$ .

The multifractal characteristics of seismic noise were estimated from one-minute data on successive time intervals with a length of one day. The estimation method is based on analyzing the fluctuations after elimination of scale-dependent trends (Kantelhardt et al., 2002). The trends were eliminated by fitting local polynomials of the eighth order. The procedure of calculating the multifractal statistics of seismic noise is described in sufficient detail in (Lyubushin, 2007; 2008a; 2009; 2010a; 2010b; 2011a; 2011b) and will not be discussed in this paper.

Thus, just as in the case of minimal normalized entropy  $En$ , the time series of  $\Delta\alpha$  and  $\alpha^*$  with a time step of 1 min were formed from the records at each station.

By its definition,  $\Delta\alpha$  is a measure of diversity in the random behavior of the signal; roughly speaking, this parameter reflects the number of the Helder–Lipschitz exponents. The simple random monofractal signal has a single Helder–Lipschitz exponent, which is at the same time the Hurst exponent as well. Therefore, the decrease in  $\Delta\alpha$  indicates that certain degrees of freedom of the system generating the studied system are suppressed, and their number is reduced. In (Pavlov and Anischenko, 2007), the phenomenon of reduction in the support width of the singularity spectrum  $\Delta\alpha$ , which

the authors termed a loss of multifractality, is studied using the time series and the models of synchronization in the behavior of nonlinear oscillators. The authors showed that, upon synchronization (owing to the enhancement of coupling between the elements of the system), parameter  $\Delta\alpha$  decreases.

## CONSTRUCTING THE MAPS OF THE STATISTICS

As the F-net network covers the entire territory of Japan (Fig. 1) and the records at each station provide the input for daily calculations of the estimates  $\Delta\alpha$ ,  $\alpha^*$ , and  $En$ , it is possible to construct daily maps of spatial variations in these parameters. For calculating a digital map, we cover the rectangular area that comprises all stations by a uniform grid of nodes. Each node with an integer-valued double index  $(i, j)$  is set in correspondence with the values  $\Delta\alpha$ ,  $\alpha^*$ , and  $En$ , which are the median values over the given number of the stations that are closest to the considered node. All the maps presented in this paper were calculated as a set of the median values of studied parameters at five stations that are closest to a given grid node. The medians were calculated at the nodes of a uniform grid covering the rectangular area confined between  $30^\circ$  and  $46^\circ$  N in latitude and  $128^\circ$  and  $146^\circ$  E in longitude and consisting of  $30 \times 30$  nodes. Averaging the daily maps over all days within a large time interval gives the average maps.

In addition, the daily medians of  $\Delta\alpha(i, j)$ ,  $\alpha^*(i, j)$ , and  $En(i, j)$  calculated at the nodes  $(i, j)$  can be bundled in the aggregated normalized map  $Ag_N(i, j)$ . In order to construct this map, we calculated the normalized values of these parameters for the maps for each day. In the case of  $\Delta\alpha$  and  $\alpha^*$ , we inverted the values in order to change their minima to their maxima:

$$\begin{aligned} \Delta\alpha_N^{(inv)}(i, j) &= (\max_{i,j} \Delta\alpha(i, j) - \Delta\alpha(i, j)) / (\max_{i,j} \Delta\alpha(i, j) - \min_{i,j} \Delta\alpha(i, j)), \\ \alpha_N^{*(inv)}(i, j) &= (\max_{i,j} \alpha^*(i, j) - \alpha^*(i, j)) / (\max_{i,j} \alpha^*(i, j) - \min_{i,j} \alpha^*(i, j)), \\ En_N(i, j) &= (En(i, j) - \min_{i,j} En(i, j)) / (\max_{i,j} En(i, j) - \min_{i,j} En(i, j)). \end{aligned} \quad (3)$$

Here, the lower index  $N$  denotes the normalizing operation, and the upper symbol “*inv*” for the parameters  $\Delta\alpha$  and  $\alpha^*$  denotes the inversion. Clearly, the quantities defined in (3) range from 0 to 1. Then, we determine the value of the aggregated normalized

map in the node  $(i, j)$  by calculating the average of the quantities in (3):

$$Ag_N(i, j) = (\Delta\alpha_N^{(inv)}(i, j) + \alpha_N^{*(inv)}(i, j) + En_N(i, j))/3, \quad 0 \leq A_N(i, j) \leq 1. \quad (4)$$

The maxima of the aggregated normalized parameter (4) correspond to the minima in  $\Delta\alpha$  and  $\alpha^*$  and to the maxima in  $En$ .

## THE RESULTS OF THE ANALYSIS

The averaged maps of  $\Delta\alpha(i, j)$ ,  $\alpha^*(i, j)$ ,  $En(i, j)$ , and  $Ag_N(i, j)$  are presented in Figs. 2 and 3 for three time intervals: from the beginning of 1997 to September 25, 2003 (maps (a)); from September 26, 2003, to March 10, 2011 (maps (b)); and from March 14, 2011 (the date of resumed operation of the F-net after the earthquake of March 11, 2011) to May 15, 2012. It can be seen in Figs. 2 and 3 that the three parameters of seismic noise considered in this work are correlated with each other. Their coefficients of pair correlation  $\rho$  calculated over all stations of the network and over the entire time interval of observations are

$$\begin{aligned} \rho(\Delta\alpha, \alpha^*) &= 0.638, \quad \rho(\Delta\alpha, En) = -0.756, \\ \rho(En, \alpha^*) &= -0.533. \end{aligned} \quad (5)$$

The high magnitudes of correlations (5) suggest the idea of a combined use (aggregation) of the noise parameters by formula (4) for identifying the regions where the minima in  $\Delta\alpha$  and  $\alpha^*$  are rendered simultaneously with the maxima in  $En$ .

The maps (a) in Figs. 2 and 3 present the spatial distributions of the studied parameters from the start of operation of the F-net network to the strong seismic event that occurred off the shore of Hokkaido on September 25, 2003. This event had the magnitude  $M = 8.3$  and, according to the interpretation suggested in (Lyubushin, 2008b; 2009), was the first strong manifestation of the revealed growing destabilization of the lithosphere within the entire region of the Japanese islands. In a certain sense, this event can be considered as a foreshock to the followed mega earthquake of March 11, 2011, and therefore, it was concluded in the middle of 2008 that the next strong earthquake would exceed magnitude 8.3.

After the earthquake of 2003, the average value of  $\Delta\alpha$  slightly (although still statistically significantly) decreased, which can be seen from the comparison of Figs. 2a' and 2b'. We note that the area of the forthcoming mega earthquake in Fig. 2a' is marked by the substantially reduction in  $\Delta\alpha$ , which indicates that the preparatory processes that resulted in the seismic catastrophe had started long before 1997, the year when the F-net network observations were launched. This is quite natural, because the expected time of occurrence of new precursors to mega earthquakes with magnitude 9 is estimated as 30–50 years before the event (Rikitake, 1976). It is remarkable that, after the earthquake of

2003, the area of reduced  $\Delta\alpha$  split into two segments (Fig. 2b), and only one segment (the northern one) actualized as a region of the earthquake.

The spatial distribution of  $\Delta\alpha$  estimated from the current data after the mega earthquake is shown in Fig. 2c'. An important feature of this distribution is that the average level of the values in this map are increased up to a level of the distribution in Fig. 2a'. Moreover, after the seismic catastrophe of March 11, 2011, the area containing the epicenter and the aftershocks of this earthquake is marked by the maximum values of  $\Delta\alpha$ , which indicates that the number of its degrees of freedom has increased.

It can be supposed that, after the event of September 25, 2003, that hit off the shore of Hokkaido, the breakup of a certain area, which had been initially one (Fig. 2a') and then split into two pieces (Fig. 2b'), brought about a situation where a strong seismic event could occur in either the northern or the southern segment of the area of low  $\Delta\alpha$ . A variety of random triggering factors actualized the northern segment, whereas the southern segment of the area remained seismically intact. Thus, a hypothesis arises that the accumulated stresses were not fully released in the seismic catastrophe of March 11, 2011, and the southern zone of reduced  $\Delta\alpha$ , which is assessed as a seismically hazardous region in the context of the suggested interpretation, poses a severe threat for the megalopolis of Tokyo, which is close to this zone (Lyubushin, 2011d; Lyubushin, Rodkin, and Tikhonov, 2011).

As far as the other noise parameters are concerned, namely, for the maps of the generalized Hurst index  $\alpha^*$  (Figs. 2a'', 2b'', and 2c''), we may almost literally repeat what has been said above about the parameter  $\Delta\alpha$ . There are some distinctions, though. For example, the region of the forthcoming catastrophe identified as the area of reduced values in Fig. 2b'' is more clearly distinguished in the map of this parameter than in Fig. 2b'. The minimal normalized entropy  $En$  in Figs. 3a', 3b', and 3c' exhibits the ability to outline, by its high values, the same areas as those outlined by the minimal values of the multifractal parameters.

Finally, the aggregated normalized parameter (4) is expected to amplify the positive prognostic abilities of the anomalies in  $\Delta\alpha$ ,  $\alpha^*$ , and  $En$  and to simultaneously suppress the noise in the averaged maps thanks to the additional smoothing in formula (4). Figures 3a'', 3b'', and 3c'' show that the parameter  $Ag$  works as efficiently as its primary components. In any case, its use does not impair the results for the islands of Japan and, if applied to the data from other regions (should any appear), the simple procedure of additional averaging (4) would probably improve the result.

A question arises: In our considerations, to what extent can we rely on the spatial distributions of seismic noise parameters within a wide rectangular area if these distributions are derived from the stations installed on the islands forming the "main diagonal" of this area (Fig. 1)? This problem, which requires

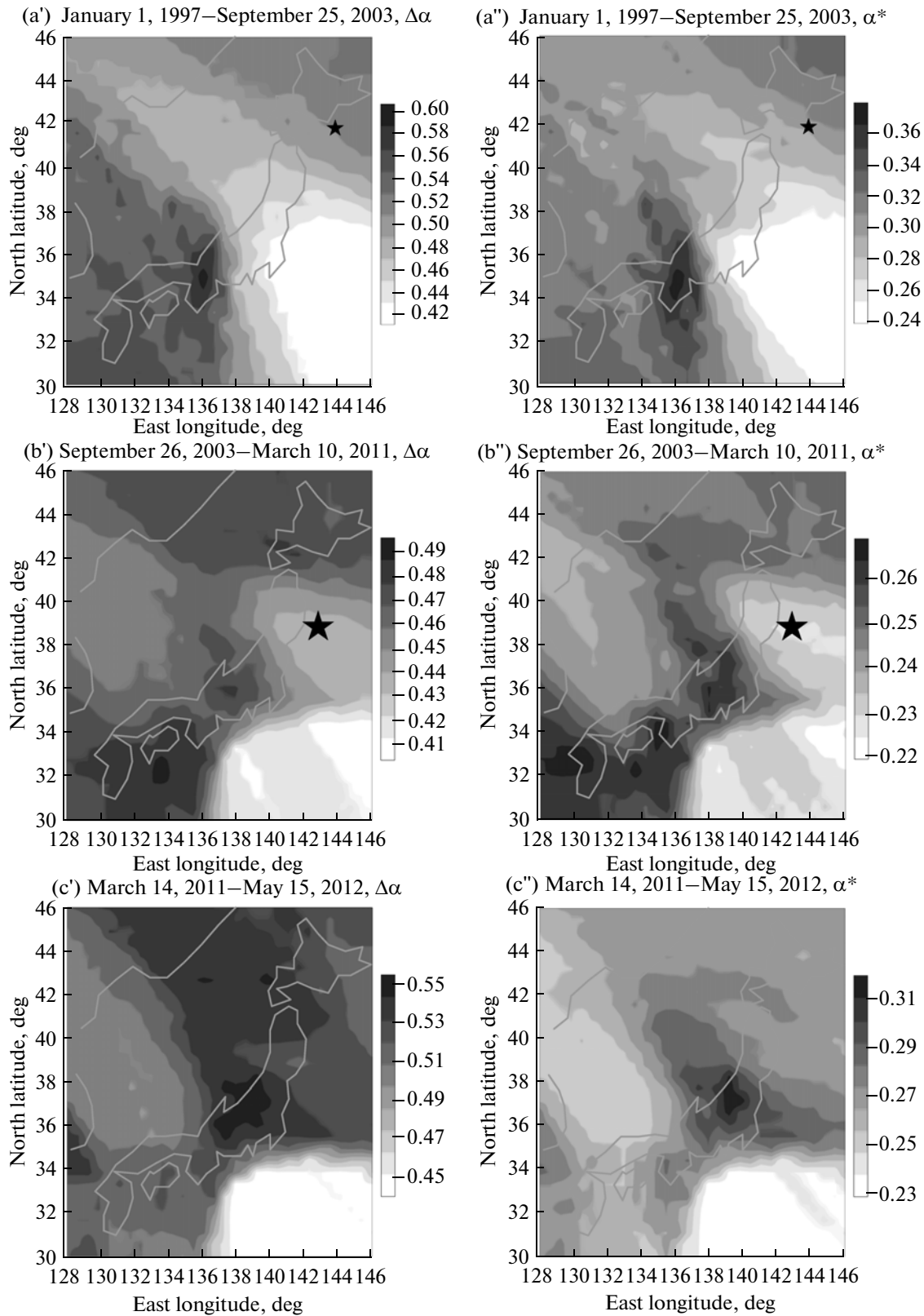


**Fig. 2.** Averaged maps showing the distributions of multifractal characteristics of seismic noise: (a', b', c')  $\Delta\alpha$  and (a'', b'', c'')  $\alpha^*$  for three successive time intervals. The asterisks correspond to the epicenters of the earthquakes that occurred on September 25, 2003 ( $M = 8.3$ ) (a', a'') and March 11, 2011 ( $M = 9.0$ ) (b', b''). The zones with the low values are interpreted as seismically hazardous regions.

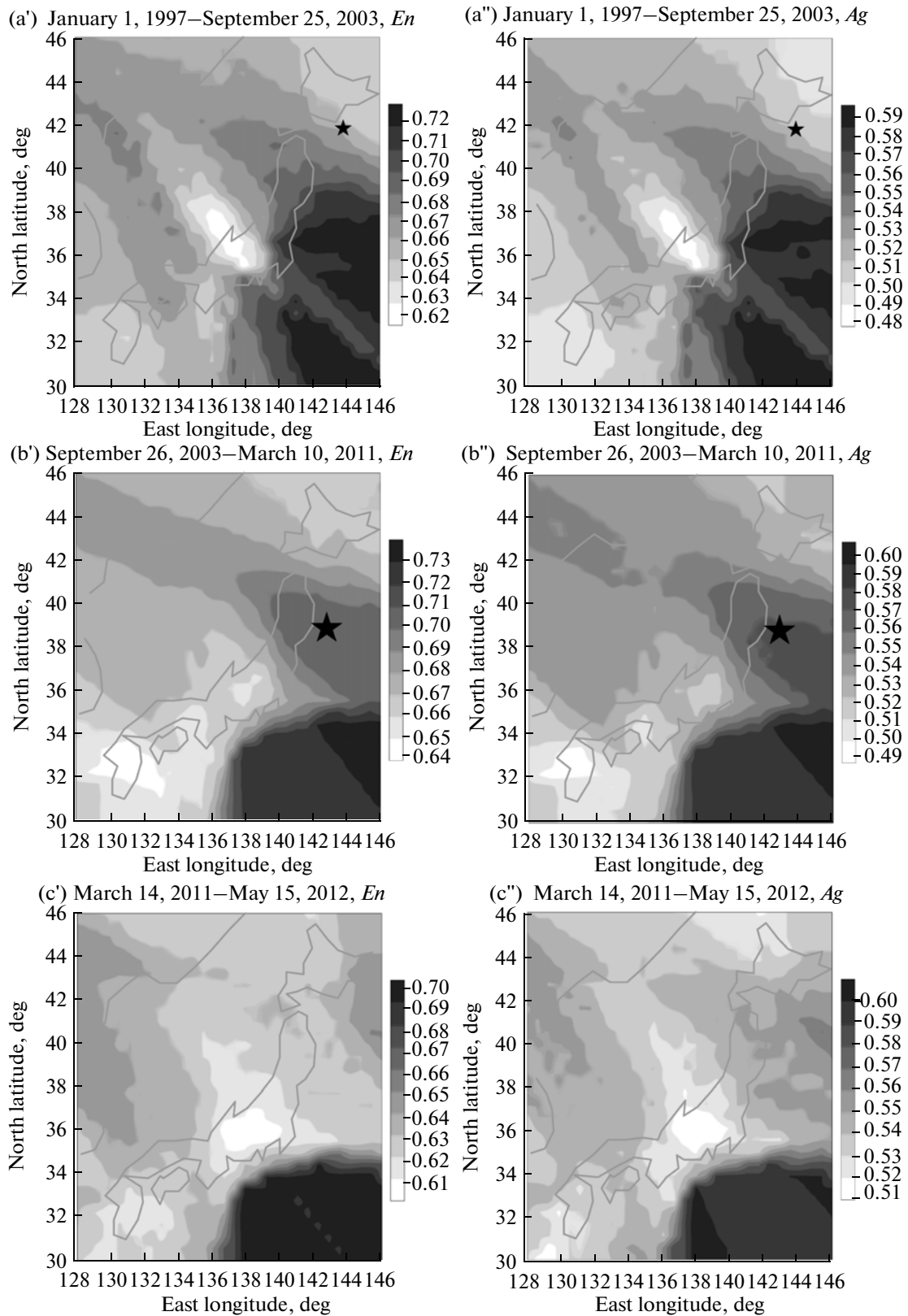


**Fig. 3.** Averaged maps showing the distributions of the minimal normalized entropy of the wavelet coefficients  $En$  and the aggregated normalized maps for  $\Delta\alpha$ ,  $\alpha^*$ , and  $En$  (a', b', c') over three successive time intervals. The asterisks correspond to the epicenters of the earthquakes that occurred on September 25, 2003 ( $M = 8.3$ ) (a', a'') and March 11, 2011 ( $M = 9.0$ ) (b', b''). The zones with the low values are interpreted as seismically hazardous regions.

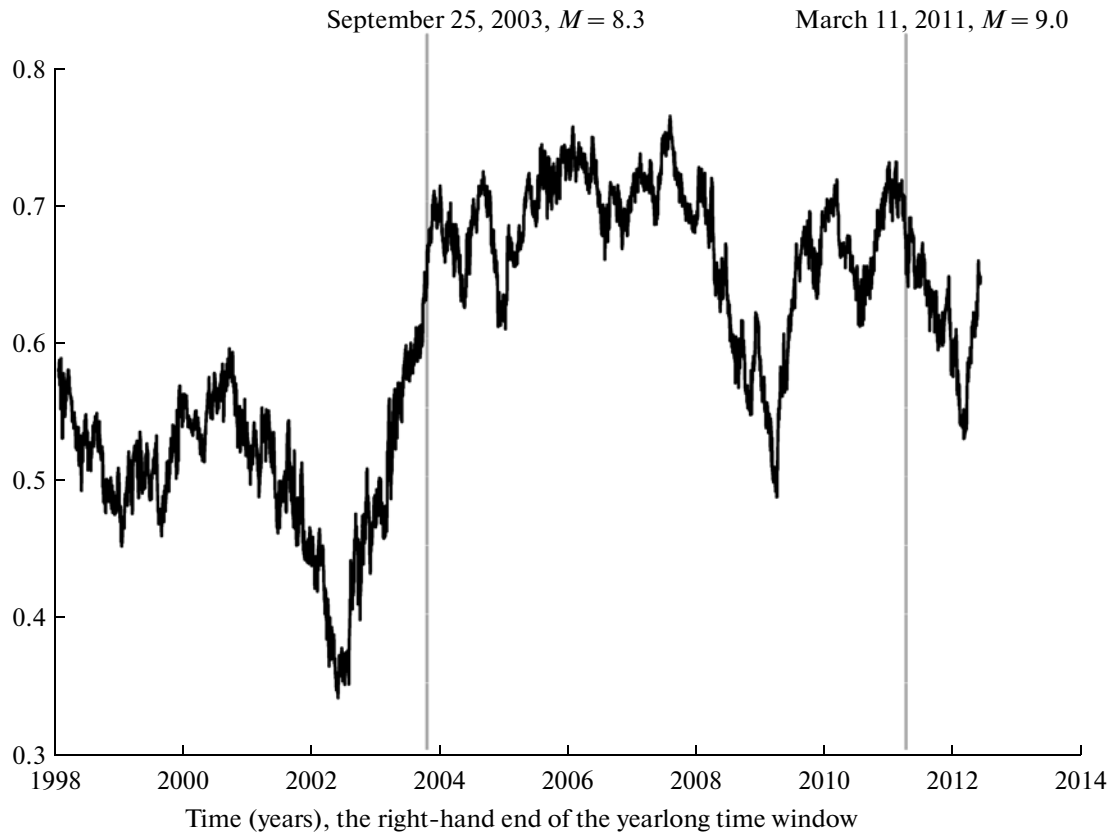


**Fig. 4.** Squared modulus of the correlation coefficient between the median daily estimates of the multifractal parameters  $\Delta\alpha$  and  $\alpha^*$  in a moving time window with a length of one year. The vertical lines mark the times of occurrence of the major earthquakes.

estimating the reliability and calculating the errors and confidence intervals, pertains to the most difficult challenges in statistics, and it would be reasonable in this respect to provide each map with a corresponding spatial distribution of standard deviations (the errors). However, consideration of these methods is far beyond the scope of the present paper. It is clear that, as the distance from the observation site increases, the values represented in the map become less reliable and their errors become larger. Therefore, we have to predicate our conclusions on the data that are available rather than on those that would be available in an ideal situation. However, the southern zone of the increased values of  $Ag_N(i, j)$  includes three seismic stations installed on small islands in the ocean (Fig. 1), and it is just the data from these stations that make the conclusions about the parameters of the noise in the left bottom corner of the considered area sufficiently well grounded.

In the general case, the multifractal parameters,  $\Delta\alpha$  and  $\alpha^*$ , are independent of each other. However, as was mentioned in formula (5) and can be seen in the maps in Fig. 2, in the case of seismic noise, these parameters are statistically correlated with each other. Figure 4 displays the graph of variations in the coefficient of correlation between the median values (over the entire net-

work) of the parameters  $\alpha^*$  and  $\Delta\alpha$ . The correlation coefficient was calculated within a moving time window with a length of one year. The remarkable feature of Fig. 4 is that the behavior of the coefficient of correlation before the mega earthquake of March 3, 2011, exhibits two striking anomalies in the form of sharp minima in 2002 and 2009. Since the first anomaly (2002) was followed by the strong earthquake on September 25, 2003, it would be reasonable to suppose that the second sharp minimum in the coefficient of correlation could also be a harbinger of a new strong seismic event to come in the second half of 2010. In terms of energy, this new event could be expected to preponderate over the earthquake of 2003. On the basis of this graph, it was suggested (Lyubushin, 2011a, submitted in April 2010) that since mid-2010, Japan has faced a threat of a new strong earthquake.

By analyzing the graph after March 11, 2011, one can notice the incipience of the third sharp minimum in the coefficient of correlation when the right-hand end of the yearlong time window falls in the beginning of 2012. By analogy with the behavior of the correlation coefficient before the two previous strongest earthquakes, it is reasonable to suggest that the second mega earthquake will hit Japan within 1.5 to 2.5 years after the time of the third acute minimum, i.e., in the second half



of 2013 or the first half of 2014. Of course, predicting the time of the forthcoming strong earthquake is the most difficult point in seismic hazard assessment owing to the triggering mechanism of generation of seismic events, and the suggested method for estimating the expected time of occurrence of the event is open for discussion and requires further validation.

## CONCLUSIONS

The method for dynamical assessment of seismic hazards is proposed. In this method, the data measured in a sufficiently dense monitoring network are used for calculating the maps reflecting spatial distributions of the parameters of low-frequency seismic noise estimated within a moving time window. The method allows tracing the origin and evolution of the “spot of threat” (e.g., the area with the maximum values in the aggregated normalized map). If the anomalous area is stable in space and time, this fact is interpreted as the emergence of a seismic threat to the region. The size of the anomalous area provides an idea on the magnitude of the forthcoming earthquake. The trends in the values marking the anomalous zone (the decrease/increase in the multifractal parameters  $\Delta\alpha$  and  $\alpha^*$  or the increase/decrease in the minimal normalized entropy of noise  $En$  and the aggregated parameter  $Ag$ ) in the context of the described method indicate the increase/decrease in the level of seismic threat.

## ACKNOWLEDGMENTS

This work was supported by the Russian Foundation for Basic Research (grant no. 12-05-00146) and the Program of State Support for Leading Scientific Schools in Russia (project “Physics and Prediction of Earthquakes” no. NSh-5583.2012.5).

## REFERENCES

Berger, J., Davis, P., and Ekstrom, G., Ambient Earth Noise: A Survey of the Global Seismographic Network, *J. Geophys. Res.*, 2004, vol. 109, p. B11307.

Feder, J., *Fractals*, New York: Plenum, 1988.

Kantelhardt, J.W., Zschiegner, S.A., Koncsienly-Bunde, E., Havlin, S., Bunde, A., and Stanley, H.E., Multifractal Detrended Fluctuation Analysis of Nonstationary Time Series, *Physica A*, 2002, vol. 316, nos. 1–4, pp. 87–114.

Kobayashi, N. and Nishida, K., Continuous Excitation of Planetary Free Oscillations by Atmospheric Disturbances, *Nature*, 1998, vol. 395, pp. 357–360.

Lyubushin, A.A. and Sobolev, G.A., Multifractal Measures of Synchronization of Microseismic Oscillations in a Minute Range of Periods, *Izv. Phys. Solid Earth*, 2006, vol. 42, no. 9, pp. 734–744.

Lyubushin, A.A., *Analiz dannykh sistem geofizicheskogo i ekologicheskogo monitoringa* (Analysis of the Data of Geophysical and Environmental Monitoring), Moscow: Nauka, 2007.

Lyubushin, A.A., Microseismic Noise in the Low Frequency Range (Periods of 1–300 min): Properties and Possible Prognostic Features, *Izv. Phys. Solid Earth*, 2008a, vol. 44, no. 4, pp. 275–290.

Lyubushin, A.A., Mean Multifractal Properties of Low-Frequency Microseismic Noise, *Proc. 31st General Assembly of the European Seismological Commission, Hersonissos, 2008*, 2008b, pp. 255–270.

Lyubushin, A.A., Multifractal Properties of Low-Frequency Microseismic Noise in Japan, 1997–2008, *Book Abstr. 7th General Assembly of the Asian Seismological Commission and Japan Seismological Society, Tsukuba, 2008*, 2008c, p. 92.

Lyubushin, A.A., Synchronization Trends and Rhythms of Multifractal Parameters of the Field of Low-Frequency Microseisms, *Izv. Phys. Solid Earth*, 2009, vol. 45, no. 5, pp. 381–394.

Lyubushin, A.A., Multifractal Statistics of the Regional and Global Fields of Low-Frequency Microseisms, *Problemy kompleksnogo geofizicheskogo monitoringa Dal'nego Vostoka Rossii. Trudy Vtoroi regional'noi nauchno-tekhnicheskoi konferentsii* (Proc. Second Regional Sci.-Tech. Conf. “Problems of Comprehensive Geophysical Monitoring in the Russian Far East”, Petropavlovsk-Kamchatsky, 2009), Chebrov, V.N., Ed., Petropavlovsk-Kamchatsky: GS RAN, 2010a, pp. 186–190.

Lyubushin, A.A., The Statistics of the Time Segments of Low-Frequency Microseisms: Trends and Synchronization, *Izv. Phys. Solid Earth*, 2010b, vol. 46, no. 6, pp. 544–554.

Lyubushin, A.A., Multifractal Parameters of Low-Frequency Microseisms, in *Synchronization and Triggering: from Fracture to Earthquake Processes*, de Rubeis, V., Czechowski, Z., and Teisserye, R., Eds., Berlin: Springer, 2010c, Ch. 15, pp. 253–272.

Lyubushin, A.A., Synchronization of Multifractal Parameters of Regional and Global Low-Frequency Microseisms, *Geophys. Res. Abstr.*, 2010d, vol. 12, p. EGU2010-696.

Lyubushin, A.A., Synchronization Phenomena of Low-Frequency Microseisms, *Proc. 32nd General Assembly of the European Seismological Commission, Montpellier, 2010*, 2010e, p. 124.

Lyubushin, A.A., Cluster Analysis of Low-Frequency Microseismic Noise, *Izv. Phys. Solid Earth*, 2011a, vol. 47, no. 6, pp. 488–496.

Lyubushin, A.A., Seismic Catastrophe in Japan on March 11, 2011: Long-Term Prediction on the Basis of Low-Frequency Microseisms, *Izv. Atmos. Ocean. Phys.*, 2011b, vol. 47, no. 8, pp. 904–921.

Lyubushin, A.A., Analysis of Low-Frequency Microseismic Noise Has Permitted to Assess Magnitude, Time and Place of the Seismic Catastrophe in Japan on March 11, 2011, *Nauka Tekhnol. Razrab.*, 2011c, no. 1, pp. 3–12.

Lyubushin, A.A., Prediction of Tohoku Seismic Catastrophe by Microseismic Noise Multifractal Properties, *2011 Fall Meet. AGU, San Francisco, 2011*, 2011d.

Lyubushin, A.A., Rodkin, M.V., and Tikhonov, I.N., On Possible Strong Aftershock in the Area of the Great Japanese Earthquake 3/11/2011, *Vestn. ONZ RAN*, 2011, vol. 3, no. NZ6001. doi: 10.2205/2011NZ000108

Mallat, S., *A Wavelet Tour of Signal Processing*, San Diego: Academic Press, 1998.

- Pavlov, A.N. and Anishchenko, V.S., Multifractal Analysis of Complex Signals, *Phys. Usp.*, 2007, vol. 50, pp. 819–834.
- Rhie, J. and Romanowicz, B., Excitation of Earth's Continuous Free Oscillations by Atmosphere-Ocean-Seafloor Coupling, *Nature*, 2004, vol. 431, pp. 552–554.
- Rikitake, T., *Earthquake Prediction*, Amsterdam: Elsevier, 1976.
- Sobolev, G.A., Microseismic Variations Prior to a Strong Earthquake, *Izv. Phys. Solid Earth*, 2004, vol. 40, no. 6, pp. 455–464.
- Sobolev, G.A., Lyubushin, A.A., Jr., and Zakrzhevskaya, N.A., Synchronization of Microseismic Variations within a Minute Range of Periods, *Izv. Phys. Solid Earth*, 2005, vol. 41, no. 8, pp. 599–621.
- Sobolev, G.A. and Lyubushin, A.A., Microseismic Impulses as Earthquake Precursors, *Izv. Phys. Solid Earth*, 2006, vol. 42, no. 9, pp. 721–733.
- Sobolev, G.A. and Lyubushin, A.A., Using Modern Seismological Data to Reveal Earthquake Precursors, *Rus. J. Earth Sci.*, 2007a, vol. 9, p. ES2005. doi: 10.2205/2007ES000220
- Sobolev, G.A. and Lyubushin, A.A., Microseismic Anomalies before the Sumatra Earthquake of December 26, 2004, *Izv. Phys. Solid Earth*, 2007b, vol. 43, no. 5, pp. 341–353.
- Sobolev, G.A., Series of Asymmetric Pulses in the Low-Frequency Range (Periods of 1–300 min) of Microseisms as Indicators of a Metastable State in Seismically Active Zones, *Izv. Phys. Solid Earth*, 2008, vol. 44, no. 4, pp. 261–274.
- Sobolev, G.A., Lyubushin, A.A., and Zakrzhevskaya, N.A., Asymmetrical Pulses, the Periodicity and Synchronization of Low Frequency Microseisms, *J. Volkanol. Seismol.*, 2008, vol. 2, no. 2, pp. 118–134.
- Sobolev, G.A., *Kontseptsiya predskazuemosti zemletryasenii na osnove dinamiki seismichnosti pri triggernom vozdeistvii* (The Concept of Predictability of the Earthquakes Based on the Dynamics of Triggered Seismicity), Moscow: IFZ RAN, 2011.
- Tanimoto, T., Um, J., Nishida, K., and Kobayashi, N., Earth's Continuous Oscillations Observed on Seismically Quiet Days, *Geophys. Res. Lett.*, 1998, vol. 25, pp. 1553–1556.
- Tanimoto, T., Continuous Free Oscillations: Atmosphere-Solid Earth Coupling, *Annu. Rev. Earth Planet. Sci.*, 2001, p. 29.
- Tanimoto, T., The Oceanic Excitation Hypothesis for the Continuous Oscillations of the Earth, *Geophys. J. Int.*, 2005, vol. 160, pp. 276–288.